

Observation of Shadowing in the Virtual-Photon Total Hadronic Cross Section on Nuclei

M. S. Goodman, M. Hall,^(a) W. A. Loomis, F. M. Pipkin, and R. Wilson
High Energy Physics Laboratory, Harvard University, Cambridge, Massachusetts 02138

and

R. K. Thornton
Tufts University, Medford, Massachusetts 02155

and

R. Hicks^(b) and T. Kirk
Fermilab, Batavia, Illinois 60510

and

J. Macallister and T. Quirk^(c)
Nuclear Physics Laboratory, Oxford University, Oxford OX1 3RH, England

and

S. C. Wright
Physics Department, The University of Chicago, Chicago, Illinois 60637

and

G. Brandenburg^(d) and C. Young^(e)
Massachusetts Institute of Technology, Cambridge, Massachusetts 02139

and

W. R. Francis^(f) and I. Kostoulas^(g)
Michigan State University, East Lansing, Michigan 48823

(Received 8 May 1981)

We have measured the total hadronic cross section of virtual photons incident on carbon, copper, and lead in the region $Q^2 = 0.01\text{--}30 \text{ GeV}^2$ and $\nu = 40\text{--}200 \text{ GeV}$. A 209-GeV/c muon beam was used as a source of virtual photons. The results indicate shadowing of the virtual photons below $Q^2 = 1 \text{ GeV}^2$ and a decrease of shadowing for $Q^2 > 3 \text{ GeV}^2$. The shadowing persists to larger Q^2 than indicated by experiments at lower ν .

PACS numbers: 13.60.Hb, 12.40.Vv

The phenomenon of shadowing has been reported for both real and virtual photons incident on nuclei.¹ Shadowing is the less than linear increase of the total hadronic cross section with nucleon number A , as if part of the nuclear matter were casting a shadow on the remainder. The magnitude and dependence of the shadowing on the square of the virtual photon mass (Q^2) has been controversial,² and shadowing has been previously studied for only low-energy virtual photons ($\nu \lesssim 15 \text{ GeV}$). The amount and kinematic behavior of the virtual-photon shadowing allows us to study the transition between the two extreme pictures of photon interactions with nucleons; namely the hadronic picture, which describes the interaction of real and low- Q^2 virtual photons, and the quark-parton model which describes the interaction of high- Q^2 virtual photons.² We have measured the Q^2 dependence of the shadowing of virtual photons and ex-

tended the measurements to much larger virtual-photon energy than previous experiments.

The experiment was performed with use of the University of Chicago cyclotron magnet (CCM) spectrometer³ at Fermilab with a 209-GeV/c negative muon beam as a source of virtual photons. Muons were scattered on targets of carbon, copper, and lead, and also from an empty target for background measurements. The target thicknesses were 20.43 g/cm² for carbon, 19.78 g/cm² for copper, and 9.73 g/cm² for lead. The CCM spectrometer (Fig. 1) was modified by the addition of a lead-glass counter array, to improve the separation of hadronic events from electromagnetic background events. The event trigger consisted of a coincidence between an incident muon signal in the beam-defining scintillators (BS), a scattered muon signature in the downstream hodoscopes (a coincidence between counter M and

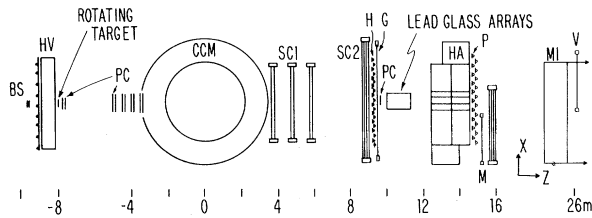


FIG. 1. The CCM spectrometer (top view): BS are beam-defining counters, HV is a halo veto wall, PC are multiwire proportional chambers, SC are spark chambers, H , G , M , and P are scintillation-counter hodoscopes, HA is a 2-m steel muon identifier, and V is the beam veto. CCM is the University of Chicago cyclotron magnet and MI is the downstream magnet iron.

counter G or H), and no signal in the downstream beam veto (V). The total muon flux was approximately 2.5×10^9 on each of the carbon and copper targets, and 4.7×10^9 on the lead target.

The analysis consisted of identifying the hadronic events and separating them from the electromagnetic background. Events were reconstructed with use of procedures developed for earlier experiments with this apparatus. The hadronic event identification utilized the quantity $\langle P_t^2 \rangle$, the average of the square of the transverse momentum of secondary particles with respect to the virtual-photon direction. For hadron secondaries, this is typically^{4, 5} $\langle P_t^2 \rangle \approx 0.18$ (GeV/c)². This is larger than the $\langle P_t^2 \rangle$ of secondaries in the more numerous electromagnetic background events due to the wide-angle bremsstrahlung process² (WAB), which is typically 0.01 (GeV/c)². The analysis divided the data into regions based on the expected shower positions of WAB photons. Events with expected shower positions outside the lead-glass aperture (events with $\nu < 110$ GeV and $Q^2 > 3$ GeV²) were assumed to be hadronic, and a calculated WAB correction was made (average $< 2\%$ all targets). For events within the lead-glass aperture, hadronic event classification was based on a variety of criteria developed from earlier studies of hadronic secondaries in this apparatus on hydrogen. These hadronic events were required to satisfy at least one of the following criteria: (a) Average P_t^2 of secondary tracks > 0.03 (GeV/c)²; (b) showers in the lead-glass array displaced out of the bending plane from the expected impact position for a WAB photon; (c) rms angular spread of spark-chamber hits upstream of the spectrometer magnet > 15 mrad with no secondary tracks downstream or detected showers. Hadronic event candidates which satisfied only one of the above

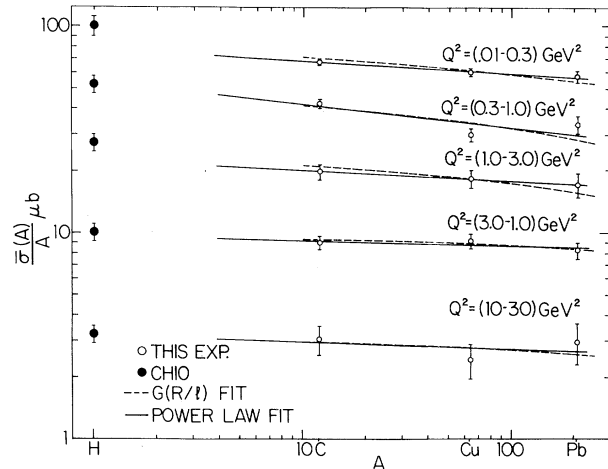


FIG. 2. Average virtual-photon total hadronic cross section for various Q^2 - ν ranges as a function of A .

conditions were further required to have a total energy deposition in the lead-glass array of $< 70\%$ of the virtual photon energy. These event-selection cuts were studied with use of Monte Carlo simulations of hadronic and electromagnetic events which were analyzed with the same procedures as the real data. The Monte Carlo calculations were based on the measured hadron distributions on hydrogen⁴ and incorporated showering of π^0 photons using the EGS code system.⁶

The total cross section for virtual photons is taken from the muon scattering cross section as

$$\sigma(Q^2, A) = \Gamma^{-1} (d^2\sigma_\mu / dQ^2 d\nu), \quad (1)$$

where Γ is the effective flux of virtual photons created by the muon. To obtain the hadronic cross sections, the data were corrected for losses of hadronic events due to event-selection cuts. These corrections were determined from ratios of event classes in the data, and checked with use of the Monte Carlo calculations.

Figure 2 shows $\bar{\sigma}(Q^2, A)/A$ for the respective targets and Q^2 ranges. The data were binned in the Q^2 region below 3 GeV² from $\nu = 110$ to 200 GeV. For the regions above 3 GeV², to improve statistics the data were binned from $\nu = 40$ to 200 GeV.

The data have been corrected for the muon acceptance of the apparatus ($> 20\%$ over the kinematic region covered), muon beam reconstruction efficiency ($> 70\%$), the loss of hadronic events ($17 \pm 5\%$ for Pb to $11 \pm 3\%$ for carbon), and the empty-target background (25% for lead to 11% for carbon). There was no correction for the radiative smear-

TABLE I. Parameter $\rho - 1$ in the fit $\bar{\sigma}(A)/A = CA^{\rho-1}$.

Q^2 (GeV ²)	$\rho - 1$	
	Expt. only	Expt. and hydrogen data
0.01 - 0.3	-0.061 ± 0.025	-0.084 ± 0.020
0.3 - 1.0	-0.113 ± 0.036	-0.107 ± 0.024
1.0 - 3.0	-0.049 ± 0.052	-0.090 ± 0.027
3.0 - 10.0	-0.023 ± 0.042	-0.030 ± 0.023
10.0 - 30.0	-0.034 ± 0.095	-0.036 ± 0.037

ing of Q^2 and ν of hadronic events. The radiative-smearing correction should not depend on nucleon number except for the shadowing effect itself. Also shown in Fig. 2 are the hydrogen data from earlier μp scattering experiments with this apparatus, where the data used are similarly uncorrected for radiative smearing and we have assigned a 10% relative normalization error to the hydrogen data. The straight lines in Fig. 2 represent power law fits to the nuclear data only. The slope parameter $\rho - 1$ of these fits is given in Table I together with those from fits which include the hydrogen data points from the earlier experiment. Values of this parameter significantly less than zero indicate shadowing. The data exhibit shadowing at low Q^2 , with and without the inclusion of the earlier hydrogen measurement.

Grammer and Sullivan² have suggested that the shadowing effect be parameterized as

$$A_{\text{eff}}/A = \sigma(A)/A\sigma(1) = G(R/l), \quad (2)$$

where A_{eff} is the effective number of nucleons participating in the interaction⁷ for a target of nucleon number A , and σ is the total hadronic virtual-photon cross section for A nucleons. The shadowing parameter G may be defined in terms of the nuclear radius R , and the virtual-photon mean free path in nuclear matter, l . We have fitted the hydrogen⁸ and nuclear cross sections with this model for the case of nuclear density, with the virtual-photon mean free path as a variable parameter. The results of these fits are given in Table II and the fit is indicated in Fig. 2. A typical hadronic mean free path in nuclear matter at these energies is ~ 2.5 fm; thus for $Q^2 < 1$ GeV² the data are consistent with hadronic behavior, whereas at large Q^2 the mean free path is larger than the nuclear diameter and the shadowing effect is diminished. The errors on l include both the systematic normalization error assigned to the hydrogen data and the statistical error in the cross-section measurements on nuclei.

TABLE II. Fitted virtual-photon mean free path [$R(\text{C}) \approx 2.6$ fm, $R(\text{Cu}) \approx 4.5$ fm, and $R(\text{Pb}) \approx 6.6$ fm].

Q^2	l	$\chi^2/\text{d.f.}$
0.01 - 0.3	$5.03^{+2.08}_{-1.20}$	1.9
0.3 - 1.0	$3.45^{+1.15}_{-0.72}$	3.2
1.0 - 3.0	$4.41^{+2.48}_{-1.25}$	0.6
3.0 - 10.0	$14.08^{+51.2}_{-6.4}$	0.3
10.0 - 30.0	$10.48^{+47.0}_{-5.41}$	0.4

Figure 3 shows A_{eff}/A for C, Cu, and Pb targets, along with results from a recent high-energy photoproduction experiment⁹ at 60 and 135 GeV,

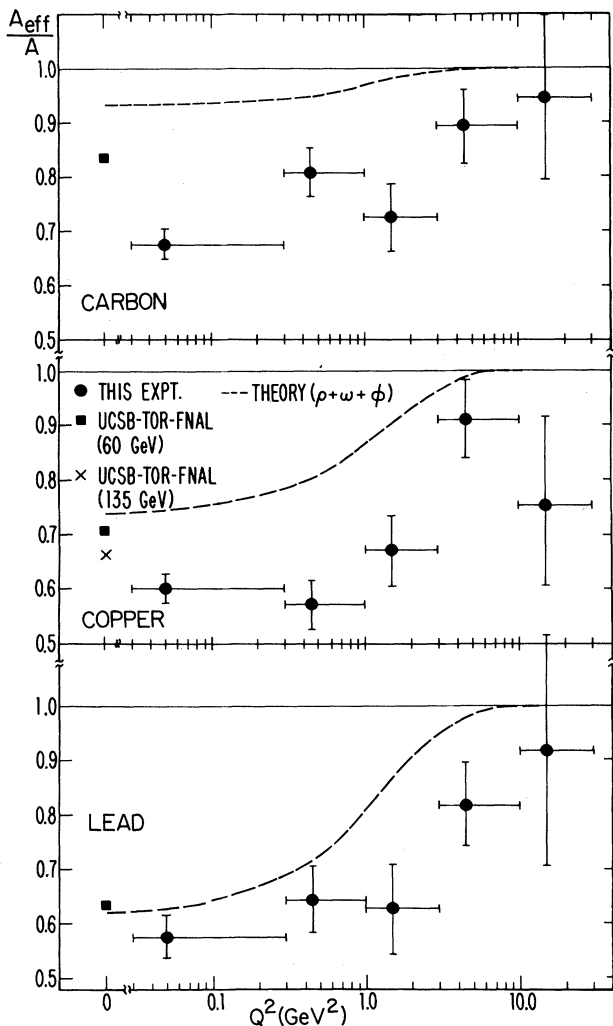


FIG. 3. A_{eff}/A as a function of Q^2 for targets of C, Cu, and Pb. Also shown are data from a high-energy photoproduction experiment (Ref. 9).

and predictions from a theoretical ($\rho + \omega + \varphi$ + pointlike) photon constituent model^{2, 10} with realistic nuclear densities. The errors shown are statistical only. We note that at high ν , the hydrogen photoproduction cross section is slowly rising, while the nuclear cross sections are decreasing as a function of ν .⁹ The shadowing effect we observe, while consistent at low Q^2 with the high-energy photoproduction result, persists to larger Q^2 than most earlier low- ν electroproduction results. However, the low- ν experiments are inconsistent among themselves.¹¹⁻¹⁵

In conclusion, we observe shadowing for $Q^2 < 1$ GeV² and observe it diminish at large Q^2 for the ν range 40–200 GeV. The shape of the data is similar to that predicted by a ($\rho + \omega + \varphi$ + pointlike) photon constituent model but the level of shadowing is larger and persists to higher Q^2 than is predicted. This suggests that mesons more massive than the ρ may participate in shadowing at these high energies.

We thank the Fermilab staff; the staff at the Rutherford Laboratory Computing Center; Dr. W. S. C. Williams of Oxford University; students S. Schochet, A. Karpovsky, and G. Denis at Harvard; and Dr. R. Milburn of Tufts University for their contributions to this work. We especially thank Dr. G. Grammer for the use of his radiative computer calculation codes and useful discussion. This work was supported in part by the U. S. Department of Energy, the National Science Foundation, and the Science Research Council (United Kingdom).

^(a)Mathematics Department, University of Wisconsin,

Madison, Wisc. 53706.

^(b)Physics Department, Vanderbilt University, Nashville, Tenn. 37235.

^(c)C.R.A. Services, Ltd., Melbourne 3001, Australia.

^(d)High Energy Physics Laboratory, Harvard University, Cambridge, Mass. 02138.

^(e)Stanford Linear Accelerator Center, Menlo Park, Cal. 94305.

^(f)Bell Telephone Laboratories, Naperville, Ill. 60540.

^(g)Hughes Aircraft Corporation, Los Angeles, Cal. 90009.

¹T. H. Bauer *et al.*, Rev. Mod. Phys. **50**, 261 (1978).

²G. Grammer, Jr., and J. D. Sullivan, in *Electromagnetic Interactions of Hadrons*, edited by A. Donnachie and G. Shaw (Plenum, New York, 1978), Vol. 2, pp. 135–351.

³B. A. Gordon *et al.*, Phys. Rev. D **20**, 2645 (1980), and Ph.D. thesis, Harvard University, 1978 (unpublished); J. Proudfoot, Ph.D. thesis, Oxford University, 1979 (unpublished).

⁴W. A. Loomis *et al.*, Phys. Rev. D **19**, 2543 (1979).

⁵J. J. Aubert *et al.*, Phys. Lett. **95B**, 306 (1980).

⁶R. L. Ford and W. R. Nelson, Stanford Linear Accelerator Center Report No. SLAC Pub. 210, 1978 (unpublished).

⁷The $n-p$ cross section difference at large ν and small x is $< 1\%$ and has been neglected in computing A_{eff} .

⁸To obtain the hydrogen cross section in the region $Q^2 < 0.3$ GeV², a fit was made to the data of Ref. 3 and included the $Q^2 = 0$ measurement of D. O. Caldwell *et al.*, Phys. Rev. Lett. **40**, 1222 (1978).

⁹D. O. Caldwell *et al.*, Phys. Rev. Lett. **42**, 553 (1979).

¹⁰G. Grammer, private communication.

¹¹J. Eickmeyer *et al.*, Phys. Rev. Lett. **36**, 289 (1976);

S. Michalowski *et al.*, Phys. Rev. Lett. **39**, 737 (1977).

¹²J. Bailey *et al.*, Nucl. Phys. **B151**, 367 (1979).

¹³S. Stein *et al.*, Phys. Rev. D **12**, 1884 (1975).

¹⁴M. May *et al.*, Phys. Rev. Lett. **35**, 407 (1971).

¹⁵M. Miller *et al.*, to be published.